Journal of Electrochemistry

Volume 13 | Issue 3

2007-08-28

Inhibition Mechanism of Imidazoline Derivate in Simulated Water from Deep Gaswell Containing CO_2

Yuan LU

He-xia LIU

Jing-mao ZHAO

Artical ID:1006-3471(2007)03-0242-07

Inhibition Mechanism of Imidazoline Derivate in Simulated Water from Deep Gaswell Containing CO_2

LU Yuan, LIU He-xia, ZHAO Jing-mao*
(*College of Materials Science and Engineering, Beijing University of Chemical Technology, Beijing* 100029, *China*)

Abstract: The electrochemical method and atomic force microscope (AFM) were applied to study the inhibition mechanism of Im-D, an imidazoline derivate inhibitor, for mild steel in CO_2 saturated solution. The imidazoline derivate can inhibit effectively CO_2 corrosion, make the steel surface smoother and belongs to the anodic controlled mixed-type inhibitor. Its adsorption on the surface of mild steel is a spontaneous and exothermic process accompanied by the decrease of entropy and follows the Langmuir adsorption isothermal equation. The lower temperature will facilitate the process. The changes in the apparent activation energy (Ea) and the pre-exponential factor (A) of the corrosion reaction before and after the addition of inhibitor were also discussed.

Key words: CO_2 corrosion; inhibitor; imidazoline derivate; AFM; Langmiur adsorption
CLC Number: **Document Code**: A

1 Introduction

CO_2 corrosion can occur at all stages of production from downhole to processing facilities and surface equipments[1-3]. In some deep gas wells being exploited in Daqing Gasfield of China, severe corrosion of oil tubes is encountered frequently due to the high partial pressure of CO_2, especially for those oil tubes located in the zone at the temperature of 60 ~ 90℃. Using inhibitors is a cost-effective and practical method of protecting materials against deterioration on account of corrosion. Some studies on the organic compounds containing nitrogen, sulfur, oxygen and phosphorus atoms indicate that they are effective corrosion inhibitors and their inhibition is attributed primarily to the adsorption of the molecules of corrosion inhibitors, via their functional group, onto the metal surface[1-2,4]. Among them, imidazoline derivates have many advantages such as high inhibition efficiency, low toxicity and easy production. There are many studies on the relationship between inhibitor adsorption and corrosion[4-9]. However, the inhibition mechanism of imidazoline derivate in CO_2-saturated solution remains poorly understood, and most researches were done by means of gravimetric measurement[10-11]. In this paper, the inhibition efficiency of an imidazoline derivate inhibition Im-D and its inhibition mechanism were studied by the weak polarization technique, AFM and Langmuir adsorption.

2 Experimental

2.1 Materials and Solution

The specimens were made from N80 oil tube with a chemical composition (%, by mass): C 0.341, Si 0.292, Mn 1.390, P 0.015, S 0.013, Cr 0.020, Mo 0.018, Ni 0.028, Al 0.033 and Fe remainder.

Received date:2007-01-11, accepted date:2007-03-12 * Corresponding author, Tel: (86-10)64442286, E-mail: jingmaozhao@126.com

Tab. 1　Chemical components of the test solution

Concentration/mg · L^{-1}	HCO_3^-	Cl^-	SO_4^{2-}	Ca^{2+}	Mg^{2+}	Na^+
	2947.50	2467.50	158.13	49.05	26.98	2677.50

Table 1 shows the chemical components of the test solution, a simulated solution of the stratum water from Daqing Gasfield. Before the test, the solution pH was adjusted to 6.5 by adding dilute HCl and the solution was deoxygenated with CO_2 for 1h. The imidazoline derivate inhibitor (Im-D) was synthesized by organic fatty acid and amine in our labariry.

2.2 Polarization Measurements

Potentiodynamic polarization tests were carried out using 273A Potentiostat/Galvanastat (EG&G Company, USA). A rod of mild steel N80 mounted into epoxy resin was used as the working electrode with an exposed area of 1cm^2, then polished with silicon carbide paper up to 1000 grit and rinsed with distilled water and degreased with acetone. After the electrode was immersed in solution for 0.5h, the potential was swept from −0.1V to 0.1V (vs. the open circuit potential) with a scan rate of 0.5mV/s. The reference electrode was a saturated calomel electrode (SCE), and the counter electrode was Pt plate.

According to the electrochemical theory[12], the weak polarization curve equation is expressed in Eq. (1).

$$i = i_{corr}\left\{\exp\frac{E-E_0}{b_a/2.303} - \frac{\exp\dfrac{-(E-E_0)}{b_c}}{1-\dfrac{i_0}{i_L}\left[1-\exp\dfrac{-(E-E_0)}{b_c/2.303}\right]}\right\} \quad (1)$$

Where b_a and b_c are the Tafel slopes of the anodic and cathodic processes; i, i_{corr} and i_L represent respectively polarization current density, the corrosion current density and the mass-transfer-controlled current density; E, E_0 are the corrosion potentials of specimens with and without the presence of inhibitor respectively.

The Gauss-Newton-Micato method was employed to fit the testing curves and the kinetic parameters of corrosion process were gained. According to Eqs. (2~4), the inhibition efficiency (η) and the anodic and cathodic interaction coefficients (f_a、f_c) can be calculated under the open circuit potential.

$$\eta = \frac{i_0 - i}{i_0} \times 100\% \quad (2)$$

$$f_a = \frac{i}{i_0}\exp[(E-E_0)/\beta_a] \quad (3)$$

$$f_c = \frac{i}{i_0}\exp[(E_0-E)/\beta_c] \quad (4)$$

2.3 Atomic Force Microscope (AFM) Examination

The rectangular specimens were N80 oil tube steel with a size of 50mm × 10mm × 30mm. Three parallel steel specimens were immersed in test solution without and with addition of 100 mg · L^{-1} Im-D. After immersed 6h, the sheets were taken out and cleaned with distilled water. After drying, the specimens were observed by Solver P47H AFM (NT-MDT Co., Russia).

3 Results and Discussion

3.1 Polarization Curves of Mild Steel in Test Solution with and without Im-D

Fig. 1 shows the potentiodynamic polarization curves of mild steel immersed in test solution containing

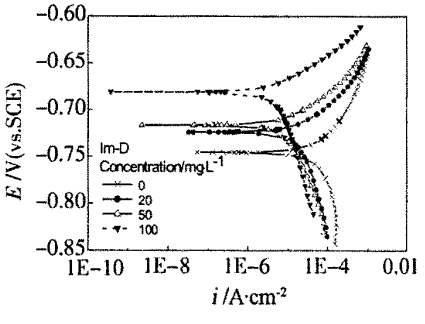

Fig. 1　Polarization curves of N80 steel in solution containing different concentrations of Im-D

Tab. 2 Electrochemical parameters and the inhibition efficiencies

[Im-D] /mg · L^{-1}	b_a /mV	b_c /mV	i_{corr} /mA · cm^{-2}	E_{corr} /mV	v_{corr} /mm · a^{-1}	f_a	f_c	Inhibition Efficiency/%
0	65.57	122.47	0.08	-745.35	0.88	—	—	—
20	46.10	580.35	0.03	-723.86	0.34	0.13	0.42	61.22
50	44.78	921.29	0.02	-716.40	0.18	0.05	0.22	79.28
100	40.73	879.15	0.01	-681.07	0.10	0.003	0.14	88.58

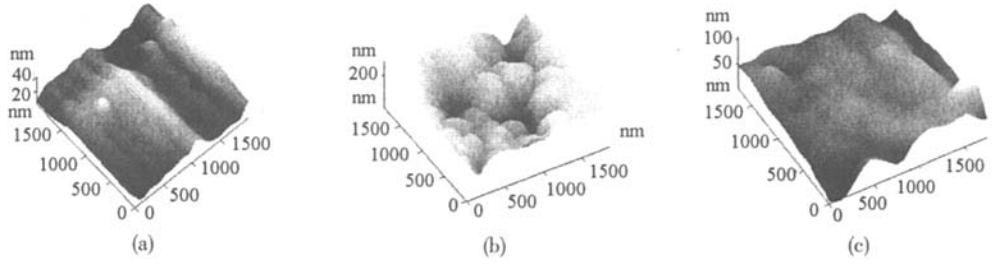

Fig. 2 AFM three-dimensional images of N80 steel surface (a) before immersion; (b) after immersion for 6h at 50 ℃ in uninhibited solution; (c) after immersion for 6h at 50 ℃ in solution containing 100 mg · L^{-1} Im-D

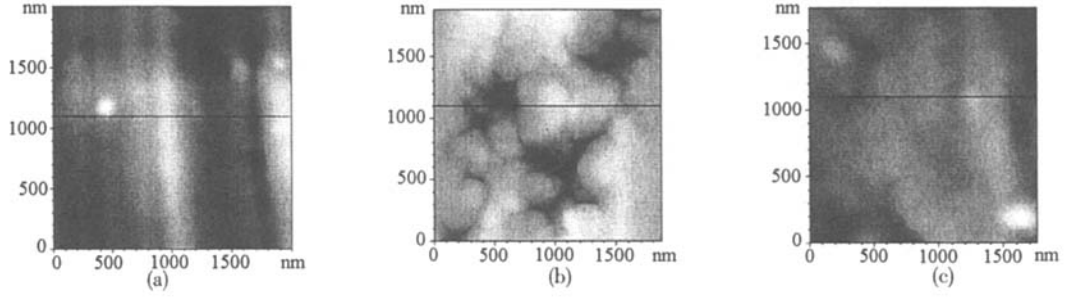

Fig. 3 AFM images of N80 steel surface topography (a) before immersion; (b) after immersion for 6h at 50℃ in uninhibited solutionL; (c) after immersion for 6h at 50℃ in solution containing 100mg · L^{-1} Im-D

different concentrations of Im-D at 50 ± 1℃. The kinetic parameters of corrosion process are listed in Table 2.

It can be seen from Fig. 1 and Table 2 that the corrosion potential goes up while both the current and the interaction coefficients decrease gradually along with increasing the concentration of inhibitor. As can be also shown, the anodic and cathodic interaction coefficients are less than 1 and the former is lower. It means that the inhibitor can more effectively retard the anodic process. Therefore, Im-D belongs to the anodic controlled mixed-type inhibitor. Its inhibition mechanism is "negative catalytic effect" according to Cao's theory[13].

3.2 Atomic Force Microscope (AFM) Observation

Fig. 2 is the three-dimensional AFM images of N80 steel surface and Fig. 3 corresponds to the steel surface topography. Fig. 2(a) and Fig. 3(a) reveal the sample before immersion is not absolute smooth which may be attributed to polishing. Fig. 2(b) and Fig. 3(b) betray that the specimen after immersion in the solution for 6 h is damaged badly. Fig. 2(c) and Fig. 3(c) display that the steel surface after immersion in solution containing 100 mg · L^{-1} Im-D is still flat and uniform relatively. Fig. 4 shows the height

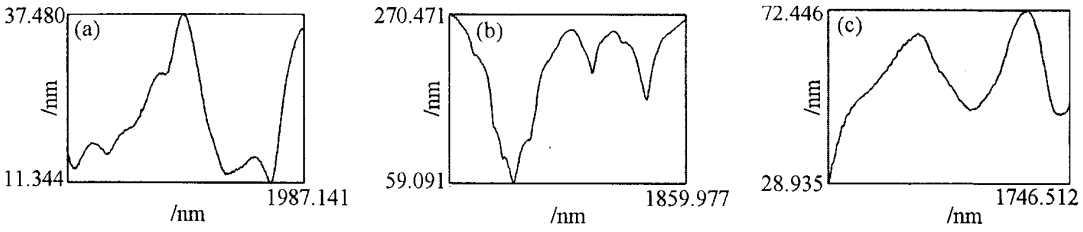

Fig. 4　Height profiles of N80 steel surface　(a) before immersion; (b) after immersion for 6h at 50℃ in uninhibited solution; (c) after immersion for 6h at 50℃ in solution containing 100mg · L^{-1} Im-D

Tab. 3　Parameters of the linear regression between C/θ and C at different temperature

Temperature /℃	Linear regression coefficient/r	Slope	Intercept /K^{-1}	Adsorptive equilibrium constant/K
25	0.99987	1.02587	6.44937	0.15505
80	0.99986	1.03580	19.39650	0.05156

profiles of mild steel surface which are made along the line marked in corresponding Fig. 3. The steel surface roughness is 26.136 nm before immersion, increases to 211.38 nm after immersion in uninhibited solution, decreases to 43.511nm when in the presence of the 100 mg L^{-1} inhibitor. These results prove that Im-D can inhibit efficiently corrosion.

3.3 Adsorption Model of Imidazoline Derivate on Mild Steel Surface

The weak polarization technique was applied to study the inhibition efficiency of the derivate at different concentration at 25 ℃ and 80 ℃ respectively. The results are shown in Fig. 5. It illustrates that the inhibition efficiency increases with the concentration of imidazoline inhibitor rising at each temperature, and keeps almost constant when the concentration is over 200 mg · L^{-1}. It is also seen that the lower the temperature is, the higher the inhibition efficiency is, which suggests that lower temperature will be helpful to adsorption of the inhibitor.

The degree of surface coverage (θ) can be calculated from Eq. (5)[14]:

$$\theta = \frac{\nu_0 - \nu}{\nu_0 - \nu_m} \tag{5}$$

Where ν_0, ν represent the corrosion rate of specimens without and with the presence of Im-D respectively; ν_m is the smallest corrosion rate.

The figure about the relationship between C/θ and C at 25 ℃ and 80 ℃ is described in Fig. 6 and the linear regression results are listed in Table 3. They indicate that C/θ and C conform to linear correlativity at 25 ℃ and 80 ℃ and the adsorption of Im-D follows the Langmiur adsorption isothermal equation, as shown in Eq. (6)[2,15-16]:

$$\frac{C}{\theta} = \frac{1}{K} + C \tag{6}$$

Where C is the inhibitor concentration, K is the adsorptive equilibrium constant.

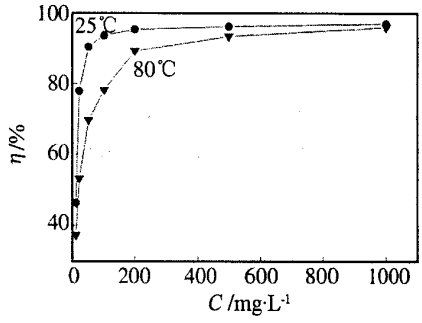

Fig. 5　Relationship between inhibition efficiency and Im-D concentration

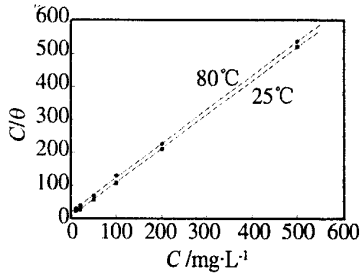

Fig. 6 Relationship between C/θ and C at different temperatures

Tab. 4 Thermodynamic parameters of adsorption of Im-D on N80 steel surface

Temperature /℃	Adsorption equilibrium constant/(K)	$\Delta H°$ /kJ · mol^{-1}	$\Delta G°$ /kJ · mol^{-1}	$\Delta S°$ /J · K · mol^{-1}
25	0.15505	-17.3692	-5.3986	-40.1496
80	0.05156	-17.3692	-3.1904	-40.1495

Tab. 5 Parameters of the regression between ln$V$ and $1/T$

Concentration of Im-D /mg · L^{-1}	Linear regression Coefficient, r	Slope /($\frac{-Ea}{R}$)	Intercept /ln(A/mm a^{-1})	Ea /KJ · mol^{-1}	A /mm · a^{-1}
0	0.99998	-0.469	1.327	3.902	3.772
20	0.97629	-1.908	4.707	15.867	110.690
50	0.98609	-2.652	6.372	22.045	585.461
100	0.99974	-2.817	6.444	23.424	628.980

3.4 Thermodynamic Parameters

The adsorption equilibrium constant (K) can be calculated in terms of the intercepts listed in Table 3. Other thermodynamic parameters ($\Delta H°$, $\Delta G°$, $\Delta S°$) were calculated approximately according to Eqs. (7), (8) and (9)[15-16]. The results are listed in Table 4.

$$\Delta H° = \frac{RT_2T_1}{T_2 - T_1}\ln(\frac{K_2}{K_1}) \quad (7)$$

$$K = \frac{1}{55.5}\exp(\frac{-\Delta H°}{T}) \quad (8)$$

$$\Delta S° = \frac{\Delta H° - \Delta G°}{T} \quad (9)$$

As can be shown by Table 4, the value of K decreases with the temperature rising, which indicates the adsorption process will be enhanced when the temperature decreases. The negative values of the adsorption heat ($\Delta H°$) suggest that the adsorption of inhibitor molecules onto mild steel surface is an exothermic process, which also proves that the lower temperature will facilitate the adsorption of inhibitor. The negative values of the adsorption free energy ($\Delta G°$) mean that adsorption is a spontaneous process. The negative values of the adsorption entropy ($\Delta S°$) imply that the process of adsorption is accompanied by a decrease in entropy. It might be interpreted in the following way: before the adsorption of inhibitor onto mild steel surface the chaotic degree of steel surface is high, however, the systemic entropy decreases when the inhibitor molecules orderly adsorbed onto the sample surface[11,15-16].

3.5 Kinetic Parameters

It has been reported by a lot of researchers that the relationship between the logarithm of the corrosion rate and the reciprocal of temperature is linear approximately for the acid corrosion of mild steel and follows Eq. (10)[11,15-17].

$$\ln\nu = \frac{-Ea}{RT} + \ln A \quad (10)$$

Where ν represents the corrosion rate; Ea represents the apparent activation energy; R represents the ideal gas constant and its value is 8.314 J · mol^{-1} · K^{-1}; T represents the temperature; and A represents the pre-exponential factor.

Fig. 7 is the relationship between lnν and $1/T$. It is found that all the regression coefficients (r) are very close to 1, which means that the linear relationship between them is good. The values of Ea and A can be calculated through the slope and intercept of the lines, and are shown in Table 5.

It's illustrated that Ea increases while A decreases when the concentration of inhibitor goes up. The increase of Ea will bring on a drop in the corrosion rate. On the contrary, the rise of A will accelerate the corrosion reaction. The value of the corrosion rate depends on them. It is believed commonly that the influence of Ea on the steel corrosion is bigger than that

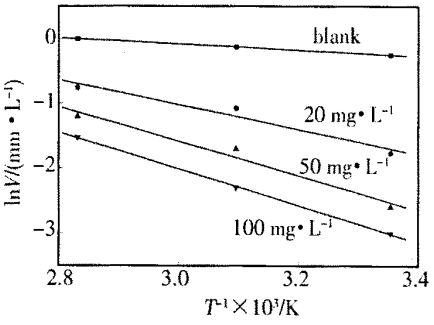

Fig. 7　Relationship between lnν and $1/T$ in solutions containing different concentrations of Im-D

of A on the steel corrosion. In the present study, Ea is the dominant factor to determine the corrosion rate. Therefore, the higher Ea in the presence of inhibitor will lead to the lower corrosion rate finally, which is consistent with the results of the electrochemical measurements.

4　Conclusions

The imidazoline derivate can protect effectively steel from CO_2 corrosion, make the steel surface roughness drop after corrosion and belongs to the anodic controlled mixed-type inhibitor. Its inhibition mechanism is "negative catalytic effect". The adsorption of inhibitor accords with the Langmuir adsorption isothermal equation. The adsorption process is a spontaneous and exothermic process accompanied by the decrease of entropy and will be accelerated at lower temperature. Higher inhibition efficiency can be obtained at lower temperature. With the increasing of inhibitor concentration, both the pre-exponential factor and the apparent activation energy increase in the present study. Ea is the dominant factor to decide the corrosion rate so that the corrosion rate reduces due to the addition of inhibitor.

References:

[1] Durnie W H, Kinsella B J, De Marco R, et al. A study of the adsorption properties of commercial carbon dioxide corrosion inhibitor formulations[J]. Journal of Applied Electrochemistry, 2001,31(11):1221-1226.

[2] Li G M. Inhition of CO_2 corrosion of carbon steel by rosin amide[J]. Anti-corrosion, 2003,50 (6):410-413.

[3] Cui Z D, Wu S L, Li C F, et al. Corrosion behavior of oil tube steels under conditions of multiphase flow saturated with super-critical carbon dioxide[J]. Materials Letters, 2004,58(6):1035-1040.

[4] Elachouri M, Hajji M S, Salem M, et al. Some nonionic surfactants as inhibitors of the corrosion of iron in acid chloride solutions[J]. Corrosion, 1996,52(2):103-108.

[5] Abd-El-Nabey B A, Khamis E, Ramadan M S, et al. Application of the kinetic-thermodynamic model for inhibition of acid corrosion of steel by inhibitors containing sulfur and nitrogen[J]. Corrosion, 1996,52(9):671-679.

[6] Zhao T, Mu G N. The adsorption and corrosion inhibition of anion surfactants on aluminium surface in hydrochloric acid[J]. Corrosion Science, 1999,41(10):1937-1944.

[7] Omanovic S, Roscoe S G. Effect of linoleate electrochemical behavior of stainless steel in phosphate buffer [J]. Corrosion, 2000,56(7):684-693.

[8] Free M L. Development and application of useful equations to predict corrosion inhibition by different surfactants in various aqueous environments[J]. Corrosion, 2002,58(12):1025-1030.

[9] Mu G N, Li X M, Li F. Synergistic inhibition between *o*-phenanthroline and chloride ion on cold rolled steel corrosion in phosphoric acid[J]. Materials Chemistry and Physics, 2004, 86(1):59-68.

[10] Zhang X Y, Wang F P, He Y F, et al. Study of the inhibition mechanism of imidazoline amide on CO_2 corrosion of armco iron[J]. Corrosion Science, 2001,43 (8):1417-1431.

[11] Mu G N, Li X M, Liu G H. Synergistic inhibition between tween60 and NaCl on the corrosion of cold rolled steel corrosion in 0.5M sulfuric acid[J]. Corrosion Science, 2005,47 (8):1932-1952.

[12] Cao C N(曹楚南). Estimation of electrochemical kinetic parameters of corrosion process by weak polarization curve fitting[J]. Journal of Chinese Society of Corrosion and Protection, 1985,5 (8):155-164.

[13] Cao C N(曹楚南). Corrosion electrochemistry[M]. Bejing: Chemical Industry Press, 1994:130-133.

[14] Sckine I, Hirakawa Y. Effect of 1-hydroxy ethylidene-1, 1-diphosphonic acid on the corrosion of SS41 steel in 0.3% sodium chloride solution[J]. Corrosion Sci-

ence, 1986,42(5):272-277.

[15] Li X H, Mu G N. Tween-40 as corrosion inhibitor for cold rolled steel in sulphuric acid: weight loss study, electrochemical characterization, and AFM[J]. Applied Surface Science, 2005,252(5):1254-1265.

[16] Tang L B, Mu G N, Liu G H. The effect of neutral red on the corrosion inhibition of cold rolled steel in 1.0M hydrochloric acid[J]. Corrosion Science, 2003,45(10):2251-2262.

[17] Yu X B, Wu Z, Huang T Z, et al. Effect of carbon addition on activation and hydrogen sorption characteristics of $TiMn_{1.25}Cr_{0.25}$ alloy[J]. Materials Chemistry and Physics, 2004,83(2-3):273-277.

咪唑啉衍生物在含 CO_2 的模拟深层气井水溶液中缓蚀机理

陆 原, 刘鹤霞, 赵景茂*

(北京化工大学材料科学与工程学院, 北京 100029)

摘要: 应用电化学弱极化法和原子力显微镜(AFM)研究了咪唑啉衍生物类缓蚀剂在模拟深层气井水溶液中对碳钢的二氧化碳腐蚀的抑制效果和缓蚀作用机理. 结果表明,在不同的实验温度下,该缓蚀剂均具有较好的缓蚀性能,属于以抑制阳极为主的混合型缓蚀剂. 该咪唑啉衍生物在碳钢表面上的吸附遵从 Langmiur 方程. 计算了该腐蚀体系热力学参数(ΔH°、ΔG°和 ΔS°)以及腐蚀反应的活化能(Ea)和指前因子(A),并解释了实验结果.

关键词: CO_2腐蚀; 缓蚀剂; 咪唑啉衍生物; AFM; Langmiur 吸附